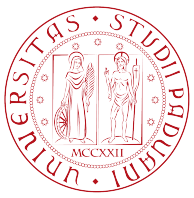

UNIVERSITÀ DEGLI STUDI DI PADOVA

SCHOOL OF ENGINEERING
DEPARTMENT OF INFORMATION ENGINEERING
SECOND CYCLE DEGREE IN AUTOMATION ENGINEERING

MASTER THESIS

Local Path Planning with Moving Obstacle Avoidance based on Adaptive MPC in ATLASCAR2

Supervisor: Prof. ANGELO CENEDESE

Co-Supervisor: Prof. VITOR SANTOS

Master Candidate: ALBERTO FRANCO

Registration Number 1156523

15th April 2019
ACADEMIC YEAR 2018/2019

Povera mente,
io ti uccido ogni giorno con le mie idee.
Povero cuore,
io ti metto alla prova ma povero me.

Ringraziamenti/Acknowledgements

dedica a parenti e amici

The research work for this thesis was carried out at the Laboratory for Automation and Robotics (LAR) in the Department of Mechanical Engineering of Aveiro (Portugal), during a period of 5 months as an exchange student.

I would like to express my gratitude to Professor Vitor Santos, for welcoming me at the Laboratory for Automation and Robotics and making possible my experience of study at the University of Aveiro. His help has been invaluable both personally and academically. Moreover I would like to thank Professor Angelo Cenedese for his advices and his help during this work.

Abstract

Inserted in the ATLASCAR2 project this work aims to develop a short-term path planning algorithm for driver assistance in dynamic environments. In order to achieve this objective, it was made a preliminary study of the existing local path planning methods and the projects that have already been developed in this field, their advantages and disadvantages were weighed and the most successful approaches applied to local navigation in real autonomous driving projects were taken into account. This thesis presents two different strategies for a self-driving car short-term path planning among multiple moving obstacles. The main task is to study and implement a motion planning and execution framework in order to make ATLASCAR2 coexist with other moving obstacle vehicles by avoiding collision and overtake them when necessary and possible. The first method developted, is an obstacle avoidance system that moves the vehicle around different moving obstacles while the second algorithm is a lane following system that keeps the ATLASCAR2 traveling along the centerline of the lanes on the road. The proposed techniques, based on the adaptive Model Predictive Control paradigm, solve optimization problems formulated in terms of cost minimization under constraints. Simulation results, developted in a MATLAB/Simulink enviroment, demonstrate and verify the feasibility and the usefulness of methods considering different scenarios, opening space for real scenario implementation.

Contents

List of Figures

Chapter 1

Introduction

In robotic research, the problem of navigation is among the most important. Basically, all autonomous mobile robots need some kind of navigation abilities to perform, localization, motion planning and guidance [6]. In the present context, we focus on navigation as a process of planning a path of a mobile robot from its current position to a desired goal location, following the planned path, and avoiding any discovered obstacles along the way. The desired paths have to fulfill several conditions to ensure safety and feasibility of the navigation. Moreover, the paths can be also defined in terms of specifications; for example, short or smooth paths are usually more desirable than long and curved ones in every dynamic environments.

Beyond the path planning, the navigation problem also involves reacting to changes of the environment model. Robots are required to move towards the target in a short time and avoid either static or dynamic obstacles observed by their sensors, which involves efficient path planning and valid obstacle avoidance.

Research and development of Unmanned Ground Vehicles has been dominated by DARPA (Defense Advanced Research Projects Agency) and NASA (National Aeronautics and Space Administration). The DARPA initiative started with the development of the first mobile robot, Shakey, and also includes the Autonomous Land Vehicle and the DARPA Demo I1 Program. NASA sponsors the development of unmanned vehicles for planetary surface exploration, from the Jet Propulsion Laboratory Mars Rover to the most recent Mars Pathfinder. Recent UGV design and development has been enhanced to build UGVs capable of operating in Intelligent Vehicle Highway Systems [7].

Over the last decades, the development of Advanced Driver Assistance Systems has become a critical endeavor to attain different objectives: safety enhancement, mobility improvement, energy optimization and comfort [8]. Much of the argument used in this discussion is based on the road mortality we see today. According to data from the World Health Organization, in 2013 there were about 1.25 million road deaths worldwide, and this number is expected to increase in the next decade [9]. Algorithms for autonomous navigation are increasingly robust and reliable and are starting to handle complex situations and decision problems.

According to Katrakazas [10], local navigation is responsible for guiding the vehicle, that is, for the planning of the direction and speed to be taken, in a space close to the current position based on information exclusively obtained by the sensors on board. The guiding must be planned in such a way as to guarantee the displacement, from the current state to the objective, without collisions.

The algorithms we have developed at the LAR, follow a new and different approach for an advanced control strategy for autonomous navigation. The idea is that these methods do not replace the algorithms developed previously but are a valid alternative, so that depending on the situation, the vehicle can choose the best strategy to overcome obstacles or solve problems that can occur on the road that need a decision in real time. Simulation results demonstrate and verify the feasibility and the usefulness of methods considering different scenarios.

In this introductory chapter, the ATLAS project is presented in more detail in section 1.1, while examples of autonomous navigation projects are discussed later (section 1.2). The context of the problem and the proposed solution of this thesis are carried out in section 1.3 while the organization of the document is discussed in section 1.4.

1.1 ATLAS Project

The ATLAS project was created in 2003 by the Group for Automation and Robotics from the Department of Mechanical Engineering at the University of Aveiro [11]. The objective of this project is to study and develop advanced sensors and active systems to promote the autonomous control of cars and other platforms. The first projects in the autonomous driving area focused on small scale models in controlled environments for participation in the National Robotics Festival (FNR) and in many other competitions winning some awards for the best performance (subsection 1.1.1). The success and experience gained with these models allowed the evolution of the project for full-scale vehicles, where ATLASCAR (subsection 1.1.2) in 2010 and ATLASCAR2 (subsection 1.1.3) in 2016 have been developed.

1.1.1 ATLAS platforms

The first developed robot (Figure 1.1a) was based on an aluminum and wood structure. In this prototype only one camera was installed that pointed to a mirror to allow the complete visualization of the road in which the robot circulated. The traction movement was assured by a mechanical differential coupled to the rear wheels and the steering movement was given by a single front wheel. In order to create a model more similar to an ordinary car, the ATLAS group developed the ATLAS 2000 (Figure 1.1b) in scale (1:4), with which it managed to win the first autonomous driving competition of the FNR in 2006. After several improvements made in ATLAS 2000, in 2008 a new platform, ATLAS MV (Figure 1.1c) was created. This robot was designed on a smaller scale (1:5), with the intention of being lighter and faster. On board were installed a new steering system, hydraulic braking and an active perception unit. This robot allowed the conquest of new victories in the autonomus driving competitions.

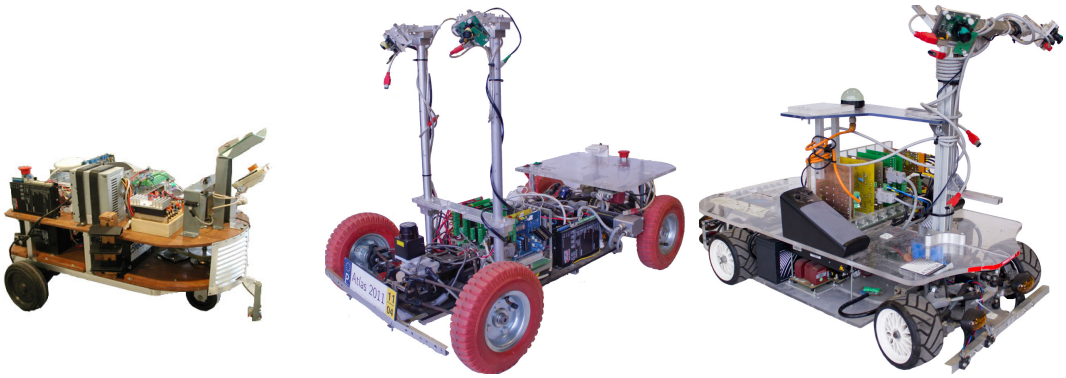

(a) First ATLAS prototype. *(b) ATLAS 2000.* *(c) ATLAS MV.*

Figure 1.1: Some of the ATLAS project small scale platforms (adapted from [1]).

1.1.2 ATLASCAR

Driven by the positive results achieved with scale models and years of navigation experience in controlled environments, in 2010 the Group of Automation and Robotics decided to invest in a large-scale project, ATLASCAR (Figure 1.2). The vehicle used for this project was a Ford Escort Station Wagon of 1998 powered by a gasoline internal combustion engine, in which several sensors, processing units and actuators were installed. On-board sensors processed data collected from the vehicle and its surroundings, with different LIDARs for obstacle detection and environmental reconstruction, pedestrian detection cameras and a Global Navigation Satellite System (GNSS) for location and route planning. After passing through the processing units, these data were sent to the actuators that allowed the movement and execution of the maneuvers in a completely autonomous way on the part of the vehicle. To power all the equipment, a Uninterruptible Power Supply (UPS) was used, loaded from an auxiliary alternator. During this project, many works were developed in the Laboratory for Automation and Robotics, many of which produced master thesis. For example, in 2014 Cabral de Azevedo [12] developed a module to detect pedestrians using sensory fusion of LIDAR and vision data while in 2016 Vieira da Silva [13] created a multisensory calibration module that was exported to subsequent projects.

Figure 1.2: The car used in ATLASCAR, based on Ford Escort Station Wagon of 1998 (adapted from [1]).

1.1.3 ATLASCAR2

Given the different limits, to continue the project, in 2016, a new vehicle was acquired: ATLASCAR2 (Figure 1.3). This time it was chosen as a platform an electric car, a Mitsubishi iMiEV, with an autonomy range of 100 km. The fact that the vehicle is electric allows to use the energy stored in the batteries, making it easier to power the sensors installed. In fact, despite the short time of existence, 3 LIDARs, a

camera, inclinometry sensors and a GNSS unit are already installed on the ATLASCAR2. Many of these sensors were transferred from ATLASCAR to this project during the work of Madureira Correia [14] in 2017, where a module for detecting free space around the car was also developed while in 2018 Ricardo Silva [2] created a local navigation module for driver assistance in the immediate decision making, identifing a solution based on a multiple hypothesis approach.

Figure 1.3: The vehicle used in ATLASCAR2, based on an electric car, a Mitsubishi iMiEV of 2015 (adapted from [2]).

1.2 Autonomous Cars

The legal definition of autonomous vehicle in the District of Columbia code is:

> *"Autonomous vehicle" means a vehicle capable of navigating District roadways and interpreting traffic-control devices without a driver actively operating any of the vehicle's control systems. The term "autonomous vehicle" excludes a motor vehicle enabled with active safety systems or driver-assistance systems, including systems to provide electronic blind-spot assistance, crash avoidance, emergency braking, parking assistance, adaptive cruise control (ACC), lane-keep assistance (LKA), lane-departure warning, or traffic-jam and queuing assistance, unless the system alone or in combination with other systems enables the vehicle on which the technology is installed to drive without active control or monitoring by a human operator.*

The modern automobile companies keep coming up with newer autonomous features in their recent models. Technological advancements seen every day in areas like information technology, communication, data analysis and storage etc. is not exclusive to these areas alone. The realm of autonomous cars is also progressing at a rapid rate these days [15]. Google's development of self-driving technology began

in January 2009. The initial objective of the project was to develop a car able to navigate on highways with minimal human intervention. In December 2016, the unit was renamed Waymo; this name derived from its mission, "a new way forward in mobility". Waymo moved to further test its cars on public roads after becoming its own subsidiary.

(a) Google's Firefly self-driving prototype in 2015 (adapted from [16]).

(b) Waymo Chrysler Pacifica Hybrid self-driving prototype in 2017 (adapted from [16]).

Figure 1.4: Some of the Waymo/Google prototypes tested across multiple locations in the Unided States in recent years.

Waymo uses LIDAR which sends out millions of laser beams per second to build up a detailed picture of the world all 360 degrees around it. It also uses radar to detect how far away objects are and their speed and high-resolution cameras detect visual information like whether a traffic signal is red or green. It then combines all that data to understand the world around it and predict what those things might do next. It can do that for things up to three football fields away. Based on all this information, Waymo's software determines the exact trajectory, speed, lane and steering maneuvers needed to progress along this route safely [16] [17].

With the advances in autonomous technology, VIAC or VisLab Intercontinental Autonomous Challenge was one of the major competitions which led to improve-

ments in the testing and analysis of autonomous vehicles and robotics. It was a 13,000 kilometers trip, nearly three months from Parma, Italy to Shanghai, China from July 20, 2010 to October 28, 2010. It involved four autonomous vehicles with negligible human intervention and high level of autonomy [18]. One of VisLab's advanced autonomous car, BRAiVE (Figure 1.5), drove in downtown Parma on July 12th, 2013. It successfully navigated narrow rural roads, crosswalks, traffic lights, pedestrian areas, roundabouts and artificial hazards. It was a pioneer in the field of vehicular robotics, since it was totally autonomous [3].

Figure 1.5: BRAiVE prototype developted by VisLab, based on a Hyundai Sonata (adapted from [3]).

Another example of autonomous system is Navya, a robotically driven electric shuttle which operates at a maximum speed of 25 kilometers per hour. Made by Induct Technology, France, it can accommodate 15 passengers. It uses four LIDAR units and stereoscopic optical cameras, and it does not require any road modifications. Its LIDAR unit and optical cameras help in generating a real-time three dimensional map of the surroundings. It is being successfully tested at various universities across Switzerland, England and Singapore [19].

Figure 1.6: Navya Shuttle developted in 2016 by Navya Group in France.

1.3 Context of the Problem and Proposed Approach

Dynamic environments pose several added difficulties to the motion planning problem. The dynamics of the ATLASCAR2 must be taken into account, and there are limitations due to the sensors range and uncertainty in measurements, that must be reflected on the motion plan. Besides it, a motion plan must incorporate time restrictions, meaning the vehicle will require a certain amount of time to accomplish a task. For example, when crossing a road, the ATLASCAR2 must do it fast enough to avoid incoming cars. The proposed algorithms were studied for the ATLASCAR2 project in which the group for Robotics and Automation at the University of Aveiro has setup and adapted a common commercial electric vehicle to provide a versatile framework to develop studies and research [11] [20]. The fact that the vehicle is electric allows to use the energy stored in the batteries, making it easier to power the sensors installed. In fact, the ATLACAR2 is equipped with sensors, such as lidar, that measure the distance to obstacles in front and around the vehicle. The obstacles can be static, such as a large pothole, or moving, such as a moving vehicle on the same or a nearby lane. The most common maneuver from the driver is to temporarily move to another lane, drive past the obstacle, and move back to the original lane afterward. In this case, we want to design an obstacle avoidance system that moves the ATLASCAR2 around moving obstacles in the lane using throttle and steering angle. This system uses an adaptive Model Predictive Controller that updates both the predictive model and the mixed input/output constraints at each control interval. Moreover we want to develop a lane-keeping assist system for the vehicle: it has a sensor, such as camera or laser, that measures the lateral deviation and relative yaw angle between the centerline of a lane and the ATLASCAR2; it also measures the current lane curvature and its derivative. Depending on the curve length that the sensor can view, the curvature in front of the vehicle can be calculated from the current curvature and its derivative. This system keeps the autonomous car travelling along the centerline of the lanes on the road by adjusting the front steering angle. The goal for lane keeping control is to drive both lateral deviation and relative yaw angle close to zero.

1.4 Thesis Outline

In this section, we outline the thesis organization:

Chapter 1 is used to introduce the thesis focus areas of autonomous vehicle technology. In particular the ATLAS project and examples of autonomous navigation projects are presented. Moreover the context of the problem and the objectives to be achieved are carried out.

Chapter 2

Chapter 2

Literature Review

[21] [11] [22] [6]

Chapter 3

Model Predictive Control

In this chapter, the theory of Model Predictive Control is discussed in detail to highlight working principle. In particular for this work we used an advanced control strategy based on this paradigm called Adaptive MPC that uses a fixed model structure, but allows the model parameters to evolve with the time.

3.1 Generic Model Predictive Control problem

Model Predictive Control (MPC), also known as Moving Horizon Control (MHC) or Receding Horizon Control (RHC), is a popular method for the control of slow dynamical systems, to generate the required control inputs that are calculated at each sampling instance k, using the current state as initial conditions to solve a finite optimal control problem. Some of the advantages of using MPC are:

- the ability to handle unstable, time variable, non-minimum phase systems;
- robustness feature with the uncertainties in the nonlinear systems;
- built in feed-forward control to handle disturbances in the processes;
- enhanced tuning features to achieve the best response including transient responses;
- the possibility to introduce constraints in a natural form;
- if the references are known in advance, they can be used in order to optimize the reference tracking.

The methodology of all the controllers belonging to the MPC family is characterized by the following strategy, represented in Figure 3.1. The future outputs for a determined horizon, called the prediction horizon, are predicted at each instant k using the process model. These predicted outputs depend on the known values up to instant k (past inputs and outputs) and on the future control signals which are those to be sent to the system and calculated. The set of future control signals is calculated by optimizing a determined criterion to keep the process as close as possible to the reference trajectory. This criterion usually takes the form of a quadratic function of the errors between the predicted output signal and the predicted reference trajectory. The control effort is included in the objective function in most cases. An explicit solution can be obtained if the criterion is quadratic, the model is linear, and there are no constraints; otherwise an iterative optimization method has to be used. Some assumptions about the structure of the future control law are also made in some cases, such as that it will be constant from a given instant. Only the current control signal is send to the process. At the next sampling instant the measured output is evaluated and the sequence is repeated and all the steps brought

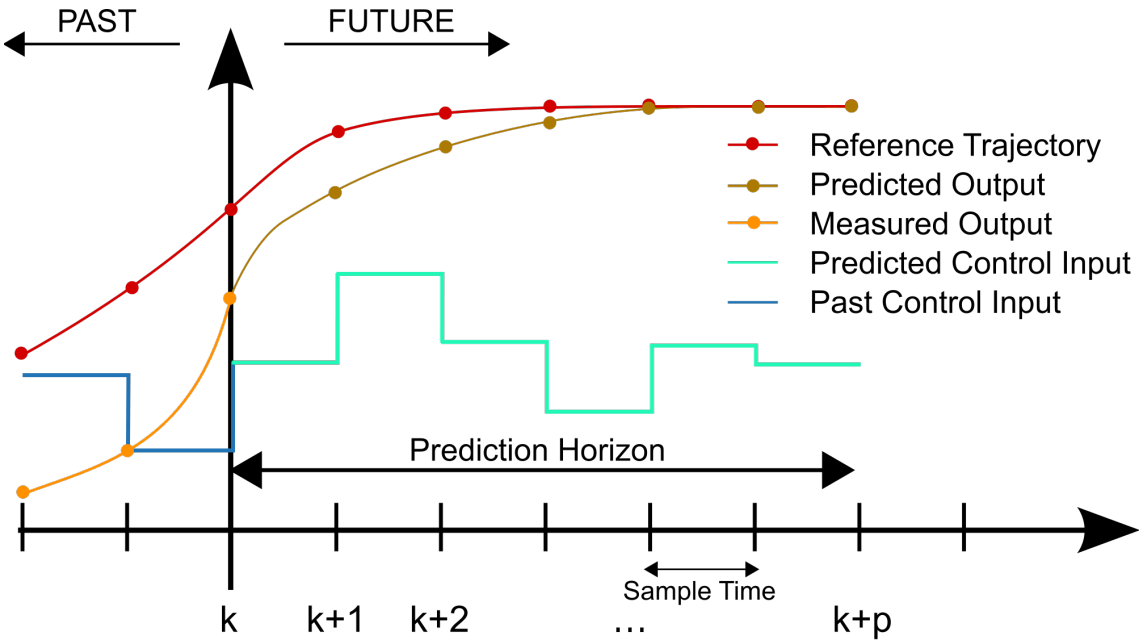

Figure 3.1: A discrete Model Predictive Control scheme adapted from [4].

up to date. Thus the predicted control input is then calculated using the receding horizon concept.

MPC is typically formulated in the state space. For a given discrete linear time-invariant (LTI) system:

$$\boldsymbol{x}(k+1) = \boldsymbol{A}\boldsymbol{x}(k) + \boldsymbol{B}\boldsymbol{u}(k) \tag{3.1}$$

where $\boldsymbol{x}(k) \in \mathbb{R}^n$, $\boldsymbol{u}(k) \in \mathbb{R}^m$ are the state and the input, respectively. The central idea in the Model Predictive Control is to minimize some cost function, while still ensuring that some constraints are fulfilled. The generic MPC problem can be written as follows:

$$\begin{aligned} \underset{\mathbf{u}}{\text{minimize}} \quad & J(\boldsymbol{x}(k), \mathbf{u}) \\ \text{subject to} \quad & \boldsymbol{x}_{k+i+1} = \boldsymbol{A}\boldsymbol{x}_{k+i} + \boldsymbol{B}\boldsymbol{u}_{k+i} \quad \forall i = 0, \dots N-1; \\ & \boldsymbol{x}_{k+i} \in \mathbb{X} \quad \forall i = 0, \dots N-1; \\ & \boldsymbol{u}_{k+i} \in \mathbb{U} \quad \forall i = 0, \dots N-1; \\ & \boldsymbol{x}_{k+N} \in \mathbb{X}_f; \quad \boldsymbol{x}_k = \boldsymbol{x}(k). \end{aligned} \tag{3.2}$$

where $\mathbf{u} = (\boldsymbol{u}_k, \dots, \boldsymbol{u}_{k+N-1})$ is a sequence of control inputs, $\boldsymbol{x}_{k+i}$ is the state at time $k+i$ as predicted at time k, and N is the prediction horizon. The sets $\mathbb{X} \in \mathbb{R}^n$ and $\mathbb{U} \in \mathbb{R}^m$ define the constraints on the state and the input, respectively. Finally, the set $\mathbb{X}_f \subseteq \mathbb{X}$ defines the terminal constraint on the state. If we consider a regulation problem, the system (3.1) should be steered to the origin and the cost function $J(\boldsymbol{x}(k), \mathbf{u})$ could be in a quadratic form as follows:

$$J(\boldsymbol{x}(k), \mathbf{u}) = \boldsymbol{x}_{k+N}^\intercal \boldsymbol{P}_f \boldsymbol{x}_{k+N} + \sum_{i=1}^{N} \left(\boldsymbol{x}_{k+i}^\intercal \boldsymbol{Q} \boldsymbol{x}_{k+i} + \boldsymbol{u}_{k+i}^\intercal \boldsymbol{R} \boldsymbol{u}_{k+i} \right) \tag{3.3}$$

where $\boldsymbol{P}_f$, $\boldsymbol{Q} \geq 0$ (positive semi-definite) and $\boldsymbol{R} > 0$ (positive definite) are weighting matrices.

Instead if we consider a servo problem, like tracking of a reference signal, the cost function is changed as follows:

$$\begin{aligned} J(\boldsymbol{x}(k), \mathbf{u}) =& (\boldsymbol{x}_{k+N} - \boldsymbol{x}^{\text{ref}}_{k+N})^\intercal \boldsymbol{P}_f (\boldsymbol{x}_{k+N} - \boldsymbol{x}^{\text{ref}}_{k+N}) \\ &+ \sum_{i=1}^{N} \Big((\boldsymbol{x}_{k+i} - \boldsymbol{x}^{\text{ref}}_{k+i})^\intercal \boldsymbol{Q} (\boldsymbol{x}_{k+i} - \boldsymbol{x}^{\text{ref}}_{k+i}) + \boldsymbol{u}^\intercal_{k+i} \boldsymbol{R} \boldsymbol{u}_{k+i} \Big) \end{aligned} \tag{3.4}$$

where $\boldsymbol{x}^{\text{ref}}_{k+i}$, $\boldsymbol{x}^{\text{ref}}_{k+N}$ describe the reference trajectory. The standard MPC algorithm can be summarized by the following steps:

Algorithm 1 Basic Model Predictive Control loop

1: Measure the current state $\boldsymbol{x}(k)$;
2: Solve the optimization problem 3.2 with $\boldsymbol{x}(k)$ as initial state, where $\boldsymbol{u}(k)$ is calculated;
3: Apply the first control of the optimal control sequence;
4: Wait one sampling time and repeat steps 1-3;

An MPC has many strengths. Given that the model is discrete and linear it handles multivariable problems very well. Also mathematical convexity is an important part of the resulting problem formulation of an MPC. In fact there exists efficient solvers for convex optimization problems but it is therefore desirable that the MPC problem 3.2 is convex which is ensured if:

1. the cost function is convex;
2. the prediction model is linear;
3. the constraint sets $\mathbb{X}, \mathbb{U}$ are convex.

The optimization handles actuator constraints and state constraints naturally in the optimization which allows for the process to be operated much closer to the hard constraints, which improves control performance and efficiency. Because of its predictive nature it is able to solve a variety of problems and handle disturbances smoothly.

3.1.1 Tuning Parameters

The two most important parameters to tune in order to satisfy the control objectives are the diagonal matrices $\boldsymbol{Q}$ and $\boldsymbol{R}$ that can be used to weight the system state matrix and the control inputs respectively. The response of the system that is too slow can be influenced by adding high weighting values in the $\boldsymbol{Q}$ matrix, whereas the control gains are damped with high weighing values in the $\boldsymbol{R}$ matrix. Find an optimal trade-off is a fundamental aspect for the constroller behaviour.

3.1.2 Stability of MPC controller

A limited horizon on the MPC problem affects the stability of the controllers; in order to avoid this problem it is possible to set an infinite horizon, impose end point constraints, terminal cost function or use other techniques. To obtain a stable controller, the parameters to tune are: the terminal cost, prediction horizon and constraints. Also the weights on the cost function can be tuned to ensure a stabilizing solution.

3.1.3 Robustness

If the stability can be guaranteed and the performance specifications are met with respect to a certain set of uncertainties, the system is said to be robust; in particular a controller with this property has to ensure that the constraints are never violated for any admissible disturbance realization. The uncertainties in a system are due to external disturbances, measurement noise, inaccurate values of the model parameters, non-linearities etc... The most common type of uncertainties considered in the literature is additive disturbance because usually the current state of the system can be measured hence there is no noise in the measurements.

3.2 Adaptive Model Predictive Control

We understood that Model Predictive Control is an advanced method that predicts future behavior using a linear-time-invariant (LTI) dynamic model. These predictions are not exact and a good strategy is to make MPC insensitive to prediction errors. If the plant is strongly nonlinear or its characteristics vary dramatically with time, MPC performance might become unacceptable because LTI prediction accuracy degrade [4]. A method that can address this degradation by adapting the prediction model for changing operating conditions is called Adaptive MPC: this control strategy uses a fixed model structure, but allows the model parameters to evolve with time. Ideally, whenever the controller requires a prediction, it uses a model appropriate for the current conditions. At each control interval, the adaptive MPC controller updates the plant model and nominal conditions. Once updated, the model and conditions remain constant over the prediction horizon. The plant model used as the basis for the adaptive MPC must be an LTI discrete-time, state-space model with a structure as follows:

$$\begin{aligned} \boldsymbol{x}(k+1) &= \boldsymbol{A}\boldsymbol{x}(k) + \boldsymbol{B}_u\boldsymbol{u}(k) + \boldsymbol{B}_v\boldsymbol{v}(k) + \boldsymbol{B}_d\boldsymbol{d}(k) \\ \boldsymbol{y}(k) &= \boldsymbol{C}\boldsymbol{x}(k) + \boldsymbol{D}_v\boldsymbol{v}(k) + \boldsymbol{D}_d\boldsymbol{d}(k) \end{aligned} \tag{3.5}$$

where the matrices $\boldsymbol{A}$, $\boldsymbol{B}_u$, $\boldsymbol{B}_v$, $\boldsymbol{B}_d$, $\boldsymbol{C}$, $\boldsymbol{D}_v$ and $\boldsymbol{D}_d$ can vary with time. The other parameters in the previous expression (3.5) are:

- k is the time index/current control interval;
- $\boldsymbol{x}$ are the plant model states;
- $\boldsymbol{u}$ are the manipulated inputs that can be adjusted by the MPC controller;
- $\boldsymbol{v}$ are the measured disturbance inputs;
- $\boldsymbol{d}$ are the unmeasured disturbance inputs;
- $\boldsymbol{y}$ are the plant outputs, including both measured (necessary at least one) and unmeasured.

In the adaptive MPC control, there are additional requirements for the plant model, like the sample time T_s that has to be constant and identical to the MPC control interval. This control strategy prohibits direct feed-through from any manipulated variable to any plant output. Thus, $\boldsymbol{D_v} = \boldsymbol{0}$ in the above model. A traditional

MPC controller includes a nominal operating point at which the plant model applies, such as the condition at which you linearize a nonlinear model to obtain the LTI approximation (equilibrium, reference trajectory and the most updated value) [4]. In adaptive MPC, as time evolves it should update the nominal operating point to be consistent with the updated plant model. It is possible to rewrite the plant model in terms of deviations from the nominal conditions as follows:

$$\begin{aligned} \boldsymbol{x}(k+1) &= \overline{\boldsymbol{x}} + \boldsymbol{A}(\boldsymbol{x}(k) - \overline{\boldsymbol{x}}) + \boldsymbol{B}(\boldsymbol{u}_t(k) - \overline{\boldsymbol{u}}_t) + \overline{\Delta \boldsymbol{x}} \\ \boldsymbol{y}(k) &= \overline{\boldsymbol{y}} + \boldsymbol{C}(\boldsymbol{x}(k) - \overline{\boldsymbol{x}}) + \boldsymbol{D}(\boldsymbol{u}_t(k) - \overline{\boldsymbol{u}}_t) \end{aligned} \tag{3.6}$$

where the matrices $\boldsymbol{A}$, $\boldsymbol{B}$, $\boldsymbol{C}$ and $\boldsymbol{D}$ are updated with respect to time. The other parameters in the previous structure (3.6) are:

- $\boldsymbol{u}_t$ is the combined plant input variable, comprising $\boldsymbol{u}$, $\boldsymbol{v}$ and $\boldsymbol{d}$ variables defined earlier;
- $\overline{\boldsymbol{x}}$ are the nominal states;
- $\overline{\Delta \boldsymbol{x}}$ are the nominal state increments;
- $\overline{\boldsymbol{u}_t}$ and $\overline{\boldsymbol{y}}$ are the nominal inputs and outputs.

The adaptive MPC uses a Kalman filter to update its controller states which include the plant, the disturbance and measurement noise model states. In particular this filter is linear-time-varying (LTV) because adjusts the gains at each control interval to maintain consistency with the updated plant model.

Chapter 4

Moving Obstacle Avoidance

In this chapter we present an Obstacle Avoidance alghorithm based on Adaptive Model Predictive Control. First we introduced the case-study model, then we designed the controller and the method of decision-making. Finally we verified the proposed strategy in different scenarios.

4.1 Problem Formulation

The collision avoidance problem is very dependent on the vehicle modeling since it is a requirement for adaptive MPC law design. Figure 4.1 illustrates a typical scenario of overtaking of a moving obstacle. The maneuver from the driver is to temporarily move to another lane, drive past the obstacle, and move back to the original lane afterward.

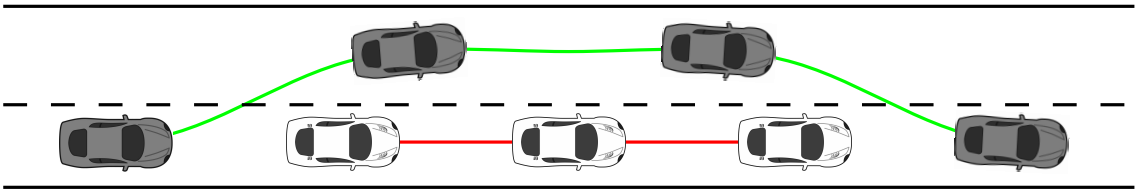

Figure 4.1: Problem description of collision avoidance on a road with only two lanes.

This is possible if and only if there is a free lane or sufficient space for overtaking the obstacle. In the case the road is busy with vehicles, the ATLASCAR2 must slow down and adapts its speed to that of the closest obstacle until the scenario changes.

4.1.1 Car-like Model

The model used in this part of the thesis should take into account the kinematic and dynamic aspects of the vehicle. Here, we present a non linear mathematical model of a vehicle used for the development of a collision avoidance system.

The model has four states and two inputs:

$$\boldsymbol{x} = \begin{bmatrix} x \\ y \\ \theta \\ v \end{bmatrix}, \qquad \boldsymbol{u} = \begin{bmatrix} T \\ \delta \end{bmatrix} \tag{4.1}$$

where (x, y) are the global coordinates of the contact point between the rear wheel and the ground, θ is the heading angle of the car body with respect to the x-axis and v is the linear speed of the car (positive). The manipulated variables are T the throttle (positive when accelerating/negative when braking) and δ the steering angle of the front wheel with respect to the vehicle (0 when aligned with

car, counterclockwise positive). Figure 4.2 illustrates the applied nonlinear bicycle model and the related parameters.

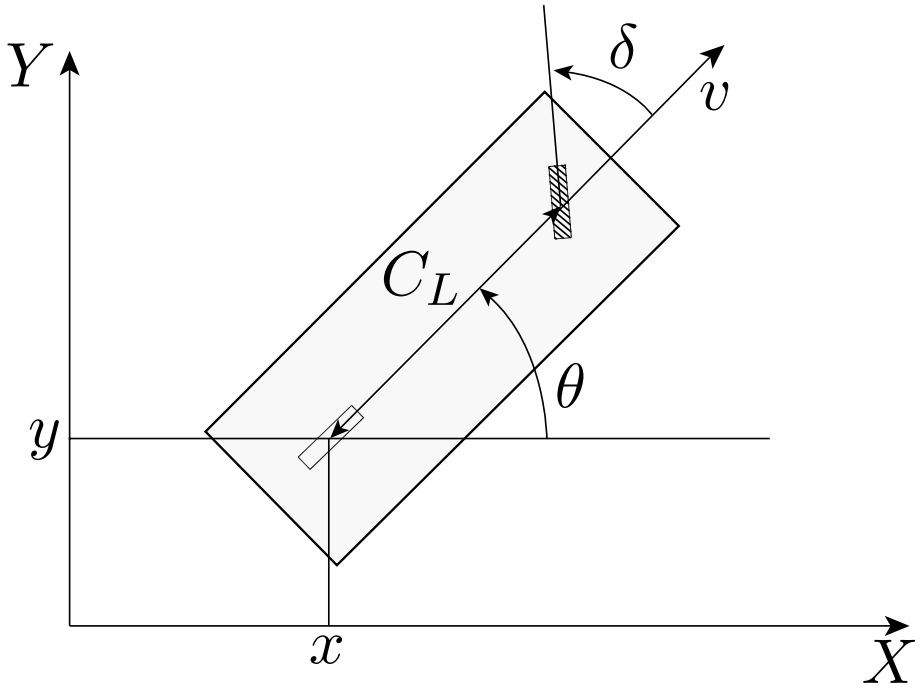

Figure 4.2: Bicycle model of a car (adapted from [5]).

The ATLASCAR2 can be modeled using the non-linear kinematic bicycle model described by the following equations of motion [23] [24]:

$$\begin{cases} \dot{x} = v\cos(\theta) \\ \dot{y} = v\sin(\theta) \\ \dot{\theta} = \dfrac{v}{C_L}\tan(\delta) \\ \dot{v} = 0.5 \cdot T \end{cases} \implies \begin{array}{l} \dot{\boldsymbol{x}} = \boldsymbol{f}(\boldsymbol{x}, \boldsymbol{u}) \\ \boldsymbol{y} = \boldsymbol{g}(\boldsymbol{x}, \boldsymbol{u}) \end{array} \tag{4.2}$$

where C_L is the car length. When the velocity is zero then the rate of change of heading angle is zero, that is, it is not possible to change the vehicle's orientation when it is not moving. If the front wheel is orthogonal to the back wheel, i.e. the steering angle is $\frac{\pi}{2}$, the ATLASCAR2 cannot move forward and the model enters an undefined region. In order to simplify the model, it is assumed that only the front wheel can be steered. Moreover, in this paper it is assumed that the ATLASCAR2 does not slip, so any slippage is thus considered as an external disturbance. Under this assumption, the slip angle is zero, meaning that the velocity is directed along the heading of the vehicle. In particular the rate of change of heading angle is referred to as turn rate which can be evaluated with a gyroscope. This yaw rate can also be deduced from the angular velocity of the wheels on the left- and right-hand sides of the vehicle which therefore rotate at different speeds because follow arcs of different radius. We can write the non-holonomic constraint which is an expression for velocity in the vehicle's y-direction in the world coordinate frame as follows:

$$\dot{y}\cos\theta - \dot{x}\cos\theta = 0 \tag{4.3}$$

This equation cannot be integrated to form a relationship between x, y and θ.

In order to use an MPC controller, the state space model needs to be linearized with a first order approximation and also re-written in a more compact form:

$$\begin{array}{l} \dot{\boldsymbol{x}} = \boldsymbol{f}(\boldsymbol{x}, \boldsymbol{u}) \\ \boldsymbol{y} = \boldsymbol{g}(\boldsymbol{x}, \boldsymbol{u}) \end{array} \implies \begin{array}{l} \dot{\boldsymbol{x}} = \boldsymbol{A}_c \boldsymbol{x} + \boldsymbol{B}_c \boldsymbol{u} \\ \boldsymbol{y} = \boldsymbol{C}_c \boldsymbol{x} + \boldsymbol{D}_c \boldsymbol{u} \end{array} \tag{4.4}$$

where the matrices $\boldsymbol{A}_c$, $\boldsymbol{B}_c$, $\boldsymbol{C}_c$ and $\boldsymbol{D}_c$ are obtained as follows:

$$\boldsymbol{A}_c = \frac{\partial \boldsymbol{f}(\boldsymbol{x}, \boldsymbol{u})}{\partial \boldsymbol{x}} = \begin{bmatrix} 0 & 0 & -v\sin(\theta) & \cos(\theta) \\ 0 & 0 & v\cos(\theta) & \sin(\theta) \\ 0 & 0 & 0 & \tan(\delta)/C_L \\ 0 & 0 & 0 & 0 \end{bmatrix},$$

$$\boldsymbol{B}_c = \frac{\partial \boldsymbol{f}(\boldsymbol{x}, \boldsymbol{u})}{\partial \boldsymbol{u}} = \begin{bmatrix} 0 & 0 \\ 0 & 0 \\ 0 & \dfrac{v}{C_L}\big(\tan(\delta)^2 + 1\big) \\ 0.5 & 0 \end{bmatrix}, \tag{4.5}$$

$$\boldsymbol{C}_c = \frac{\partial \boldsymbol{g}(\boldsymbol{x}, \boldsymbol{u})}{\partial \boldsymbol{u}} = \mathbf{I}_4, \qquad \boldsymbol{D}_c = \frac{\partial \boldsymbol{g}(\boldsymbol{x}, \boldsymbol{u})}{\partial \boldsymbol{u}} = \mathbf{0}_{4\times 2}.$$

The simple linearized approximation of the system to describe the dynamics of the ATLASCAR2 will be evaluated at the operating conditions. Note also that the system we are considering is a linear state-space model whose dynamics vary as a function of certain time-varying parameters. The system to be controlled is usually modeled by a discrete state-space model in the MPC literature. Therefore, (4.4) is transformed into a discrete state-space model to be used by the Model Predictive Controller:

$$\begin{array}{l} \dot{\boldsymbol{x}} = \boldsymbol{A}_c \boldsymbol{x} + \boldsymbol{B}_c \boldsymbol{u} \\ \boldsymbol{y} = \boldsymbol{C}_c \boldsymbol{x} + \boldsymbol{D}_c \boldsymbol{u} \end{array} \implies \begin{array}{r} \boldsymbol{x}(k+1) = \boldsymbol{A}_d \boldsymbol{x}(k) + \boldsymbol{B}_d \boldsymbol{u}(k) \\ \boldsymbol{y}(k) = \boldsymbol{C}_d \boldsymbol{x}(k) + \boldsymbol{D}_d \boldsymbol{u}(k) \end{array} \tag{4.6}$$

where $\boldsymbol{A}_d$ and $\boldsymbol{B}_d$ are the state and control matrices for the discrete state-space equation, respectively, which can be calculated with the Euler method as

$$\boldsymbol{A}_d = e^{\boldsymbol{A}_c T_s}, \qquad \boldsymbol{B}_d = \int_{kT_s}^{(k+1)T_s} e^{\boldsymbol{A}_c[(k+1)T_s - \eta]} \boldsymbol{B}_c d\eta \tag{4.7}$$

where T_s is the sampling interval for the discrete state-space model. The matrices $\boldsymbol{C}_d$ and $\boldsymbol{D}_d$ are equivalent to those in the continuous case. For simplicity, we assume that all the states are measurable and the ATLASCAR2 drives east with a constant speed at the nominal operating point. In the scenario that we are going to consider, the road is straight and our vehicle stays in the middle of the center lane when not passing. Without losing generality, the ATLASCAR2 passes an obstacle both to the right and to the left lane depending on where it is placed on the road. We create also a safe zone around the obstacles so that the vehicle does not get too close to the obstacle when passing it.

4.2 Design of Adaptive Model Predictive Control

We designed a Model Predictive Controller that can make the ATLASCAR2 maintain a desired velocity and stay in the middle of center lane. We used an Adaptive

MPC controller because it handles the nonlinear vehicle dynamics more effectively than a traditional MPC controller; in fact, the latter uses a constant plant model but the former allows us to provide a new plant model at each control interval. Because the new model describes the plant dynamics more accurately at the new operating condition, an adaptive MPC controller performs better than a traditional MPC controller. In practice, at each control interval, the adaptive MPC controller updates the plant model and the nominal conditions. Once updated, the model and the conditions remain constant over the prediction horizon. In motion planning that uses adaptive MPC, it is common to formulate the constrained control problem as a real-time optimization problem subject to hard constraints on plant variables and soft constraints on outputs; at the beginning, we specified the constraints for the manipulated variables: to prevent the ATLASCAR2 from accelerating or decelerating too quickly, we added an hard constraint on the throttle rate of change and another one on the steering angle rate of change. We used an approach that takes advantage of the ability of MPC to handle constraint explicitly. Figure 4.3 shows a conditional state machine designed for higher-level behavior planning.

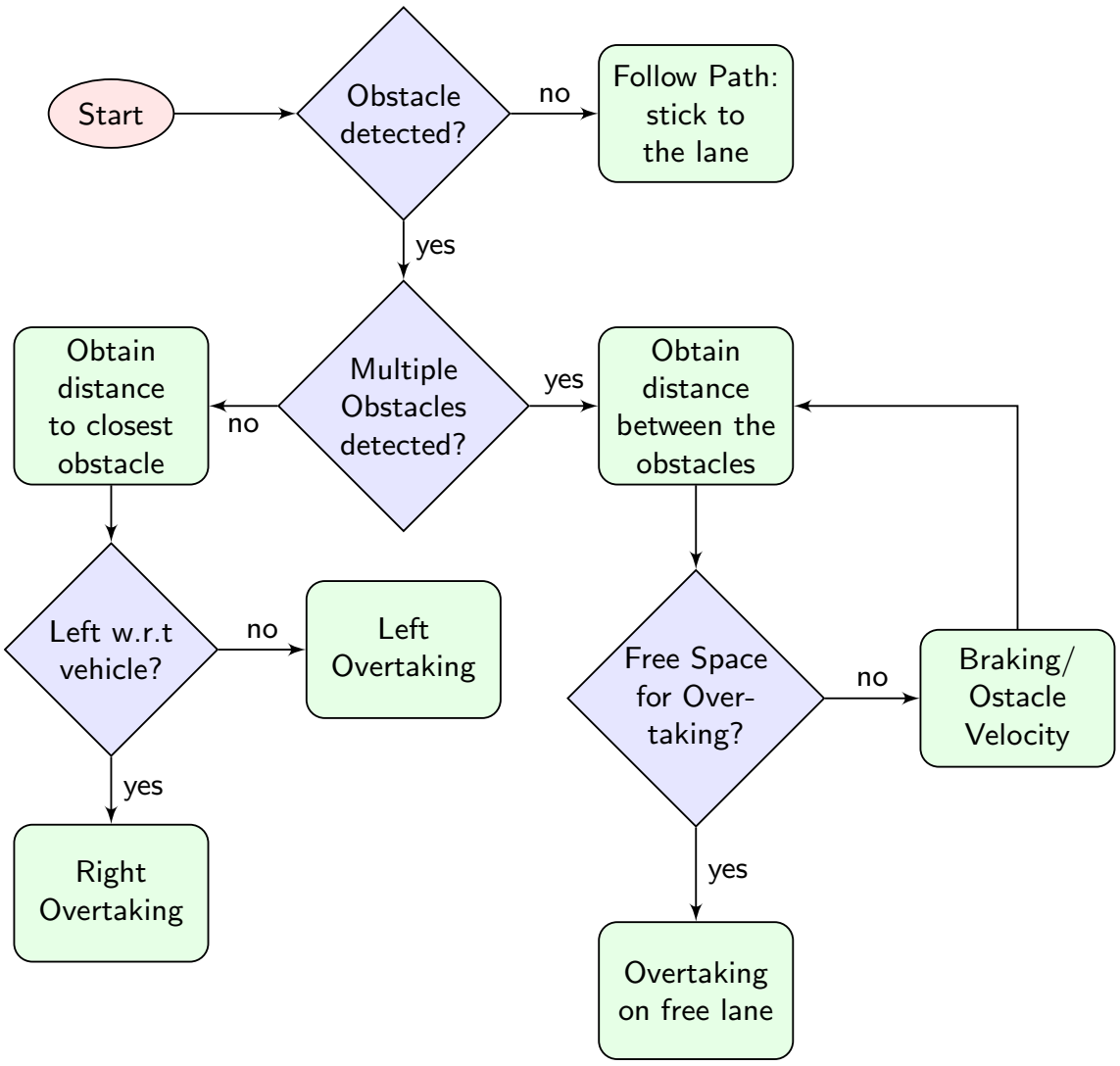

Figure 4.3: Behaviour planning conditional flowchart.

When an obstacle is detected, it defines an area on the road (in terms of con-

straints) that the ATLASCAR2 must not enter during the prediction horizon. At the next control interval the area is redefined based on the new positions of the vehicle and the obstacle until passing is completed. To define the area to avoid, we used the following mixed Input/Output constraints:

$$\boldsymbol{E}\boldsymbol{u} + \boldsymbol{F}\boldsymbol{y} \leq \boldsymbol{G} \tag{4.8}$$

where $\boldsymbol{u}$ and $\boldsymbol{y}$ are respectively the manipulated variable vector and the output variable vector, while $\boldsymbol{E}, \boldsymbol{F}, \boldsymbol{G}$ are the constraint matrices that can be updated when the controller is running. Five constraints were defined:

1. upper bound on the y-coordinate (left boundary of the road);
2. lower bound on the y-coordinate (right boundary of the road);
3. constraint for obstacle avoidance; although no obstacle is considered in the nominal condition, we must add this virtual constraint here because we cannot change the dimensions of the constraint matrices at run time;
4. upper bound on the x-coordinate (position of the closest obstacle);
5. lower bound on the x-coordinate (position of the ATLASCAR2).

The matrices for the above inequality are the following:

$$\boldsymbol{E} = \begin{bmatrix} 0 & 0 \\ 0 & 0 \\ 0 & 0 \\ 0 & 0 \\ 0 & 0 \end{bmatrix}, \qquad \boldsymbol{F} = \begin{bmatrix} 0 & 1 & 0 & 0 \\ 0 & -1 & 0 & 0 \\ cS & -1 & 0 & 0 \\ 1 & 0 & 0 & 0 \\ -1 & 0 & 0 & 0 \end{bmatrix}, \qquad \boldsymbol{G} = \begin{bmatrix} W/2 \\ W/2 \\ -cI \\ x_{\max} \\ x_{\min} \end{bmatrix} \tag{4.9}$$

where W is the width of the road, cI and cS are the required parameters such that the ATLASCAR2 must be above the line formed from the vehicle to safe zone corner for left/right passing and finally $x_{\max}$ represents the position of the closest obstacle in the case there is not free space for the overtaking (otherwise $x_{\max} = +\infty$) while $x_{\min}$ depicts the location of our vehicle. Figure 4.4 illustrates the constraints that are computed at each T_s in the case of a left overtaking.

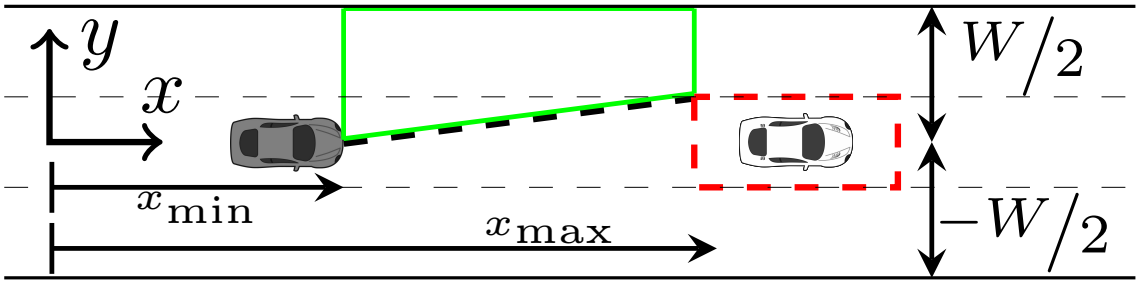

Figure 4.4: Constraints in the case of left overtaking.

4.3 Simulation Results

The performances of the proposed adaptive MPC based vehicle control method are demonstrated in three simulation examples. We tried to choose parameters that were as close as possible to a real situation: the sampling time used in the discretization of the system is $T_s = 0.02\,\text{s}$ while the values of the prediction and the control horizon are respectively $p_H = 25$ and $c_H = 5$. In all simulations, the distance between the front and rear axles is $C_L = 5\,\text{m}$ and the width of the vehicle is $C_W = 2\,\text{m}$. The saturation ranges of the control inputs are: the steering angle lies in $\left[-\frac{\pi}{30}, +\frac{\pi}{30}\right]$ rad/s while in order to prevent the ATLASCAR2 from accelerating or decelerating too quickly, we impose an hard constraint of $2.5\,\text{m/s}^2$ on the throttle rate of change. Moreover we are using a constant reference signal for the velocity of $v = 20\,\text{m/s}$ ($\approx 72\,\text{km/h}$). Blue paths in Figures 4.5, 4.7, 4.8 are known only at the end of the simulations.

4.3.1 One Moving Obstacle - Right Overtaking

In this first simulation (Figure 4.5) the ATLASCAR2 drives in the middle of the center lane while the road is completely free and when there is an obstacle, the vehicle passes it only using the right lane (the same simulation can be launched so that the car goes over to the left fast lane). In other words if the ATLASCAR2 is already in the adjacent lane, it uses the safety zone as the constraint, otherwise the vehicle must be above the line formed from the ATLASCAR2 to safe zone corner for right passing. If the vehicle is parallel to the obstacle, it uses the safety zone as the constraint and finally if it has passed the obstacle, it uses the inactive constraint to go back to the center lane. Algorithm 2 summarizes the main steps to compute custom constraints for the obstacle; when the vehicle detects the obstacle, the constraints are computed. In this simulation only the first three constraints are necessary because there is space for the overtaking without braking (the fourth and fifth constraints don't change).

4.3.2 Multiple Moving Obstacles

For a second test, additional obstacles were added to make the scenario more complex (Figure 4.7).

The vehicle is capable of overtaking the obstacles on the right or left depending on their positions with respect to the road. If the y-coordinate of the closest obstacle is greater than 0, then the vehicle overtakes to the right, otherwise the overtaking takes place on the left lane. We also hypothesized that the obstacles move at different speeds but that they are initially at a common distance; they can have a uniform motion or a uniformely accelerated motion. In case two obstacles are too close during the simulation and their distance is less than the detection range, which is 30 m, the ATLASCAR2 perceives the objects as a single entity and adapts to the situation. The same test can be done with the obstacles that drive in the same direction as the vehicle but to better assess and demonstrate results we decided to show a very unusual scenario.

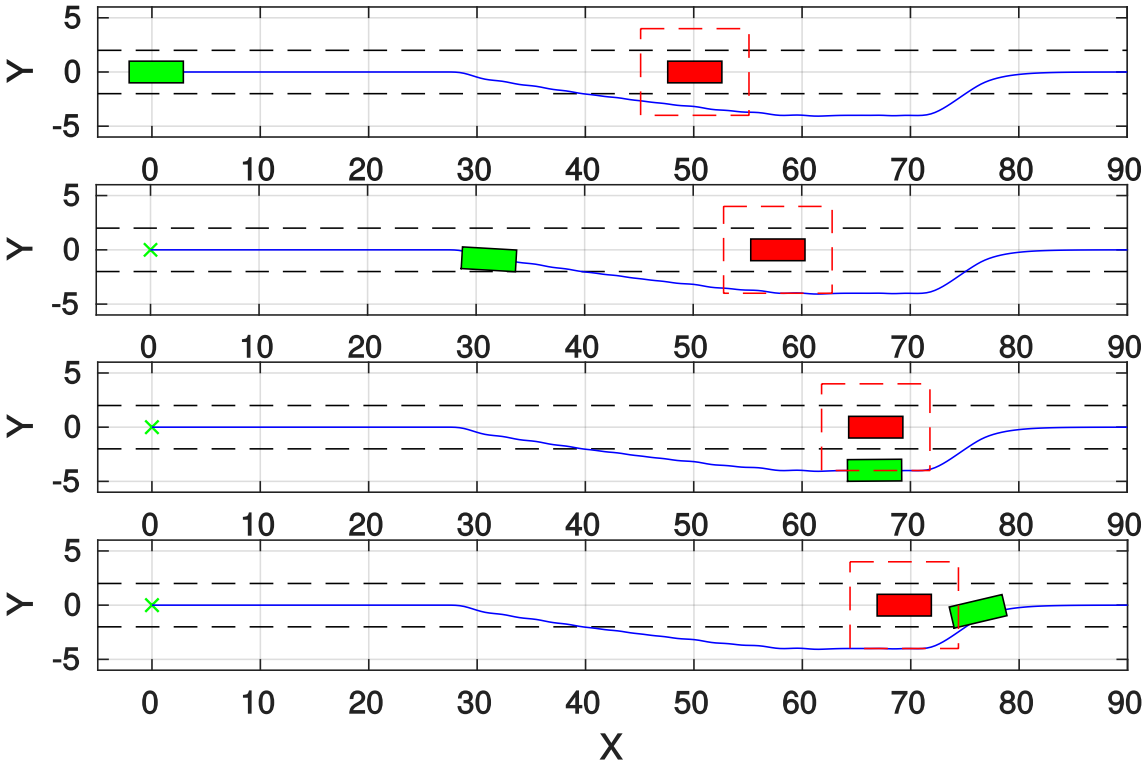

Figure 4.5: Simulation of right overtaking with one moving obstacle that moves in the same direction as the vehicle.

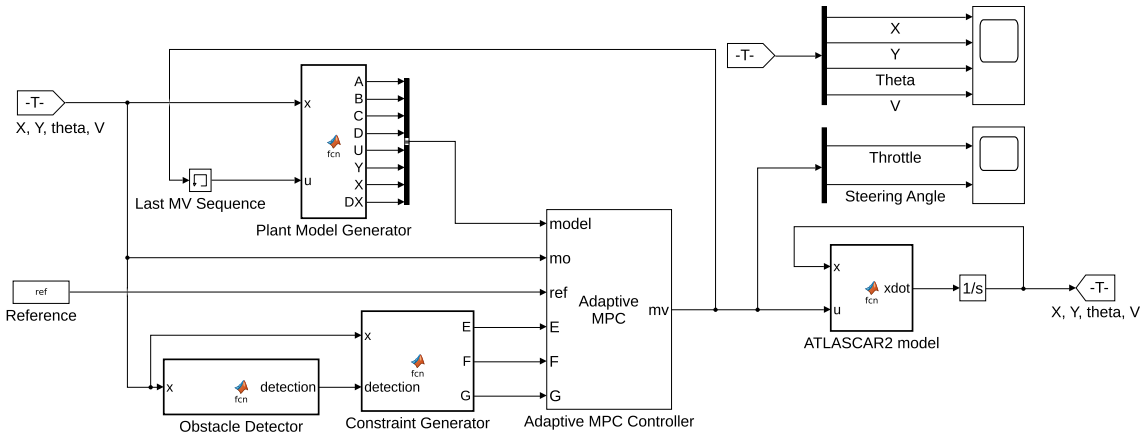

Figure 4.6: Overall procedure scheme moving obstacle avoidance.

4.3.3 Vehicle Braking and Obstacles Overtaking

Finally we have improved the code related to the mixed Input/Output constraints so that in the case there are 3 obstacles that block the road and drive at a lower speed than the ATLASCAR2, the velocity of the vehicle decreases in order to prevent the collision. Figure 4.8 depicts a simulation in which there are 3 obstacles at the same x-coordinate. Two obstacles have a constant speed of 8 m/s while the one on the left lane of 15 m/s. In this particular case it is essential to consider the fourth and the fifth restriction in order to allow the ATLASCAR2 to slow down without colliding with the cars in front. The fifth constraint is simply the position of the ATLASCAR2 that updates at each interval, while the fourth constraint, until there is a free lane, is the position of the closest obstacle (both the positions are with

Algorithm 2 Right Overtaking if an obstacle is detected

function RIGHTOVERTAKING(car, obstacle, road)
  $x_{\min} \leftarrow \text{car}X$, $x_{\max} \leftarrow +\infty$;
  obsYrr = obstacle.RearRightSafeY;
  obsXrr = obstacle.RearRightSafeX;
  if ATLASCAR2 is behind the obstacle **then**
    if ATLASCAR2 is in the adjacent lane **then**
      $cS \leftarrow 0$; $cI \leftarrow$ obsYrr;
    else
      $cS \leftarrow \tan(\text{atan2}(\frac{\text{obsYrr} - \text{carY}}{\text{obsXrr} - \text{carX}}, 1))$;
      $cI \leftarrow \text{obsYrr} - cS * \text{obsXrr}$;
    end if
  else
    if ATLASCAR2 is parallel to the obstacle **then**
      $cS \leftarrow 0$; $cI \leftarrow$ obsYrr;
    else
      $cS \leftarrow 0$; $cI \leftarrow W/2$;
    end if
  end if
  return $x_{\min}$, $x_{\max}$, cI, cS
end function

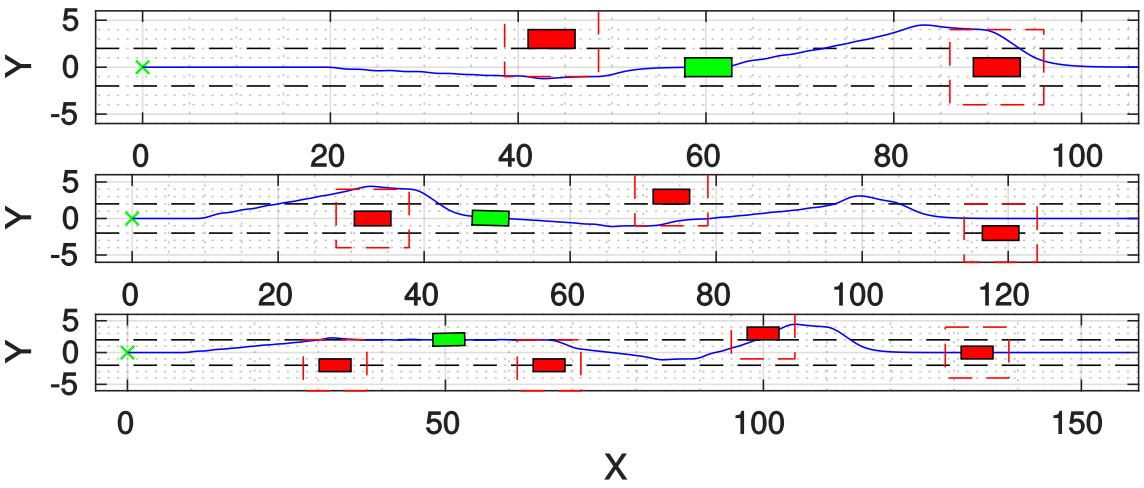

Figure 4.7: Simulations of overtaking with $N = 2, 3, 4$ moving obstacles that drive in the opposite direction with respect to the ATLASCAR2.

respect to the global reference frame). In the calculation of the fourth constraint is necessary to consider the speed at which the vehicle and the obstacle are moving in order to keep a safe distance. In particular three parameters have been identified as the key factors computing the safe distance between cars:

- detection range of the ATLASCAR2;
- velocities of the vehicle and the obstacle;
- distance between the cars.

At the beginning, the vehicle moves with the reference velocity of $v = 20\,\text{m/s}$. When the ATLASCAR2 detects all the other cars on the road, checks if there is

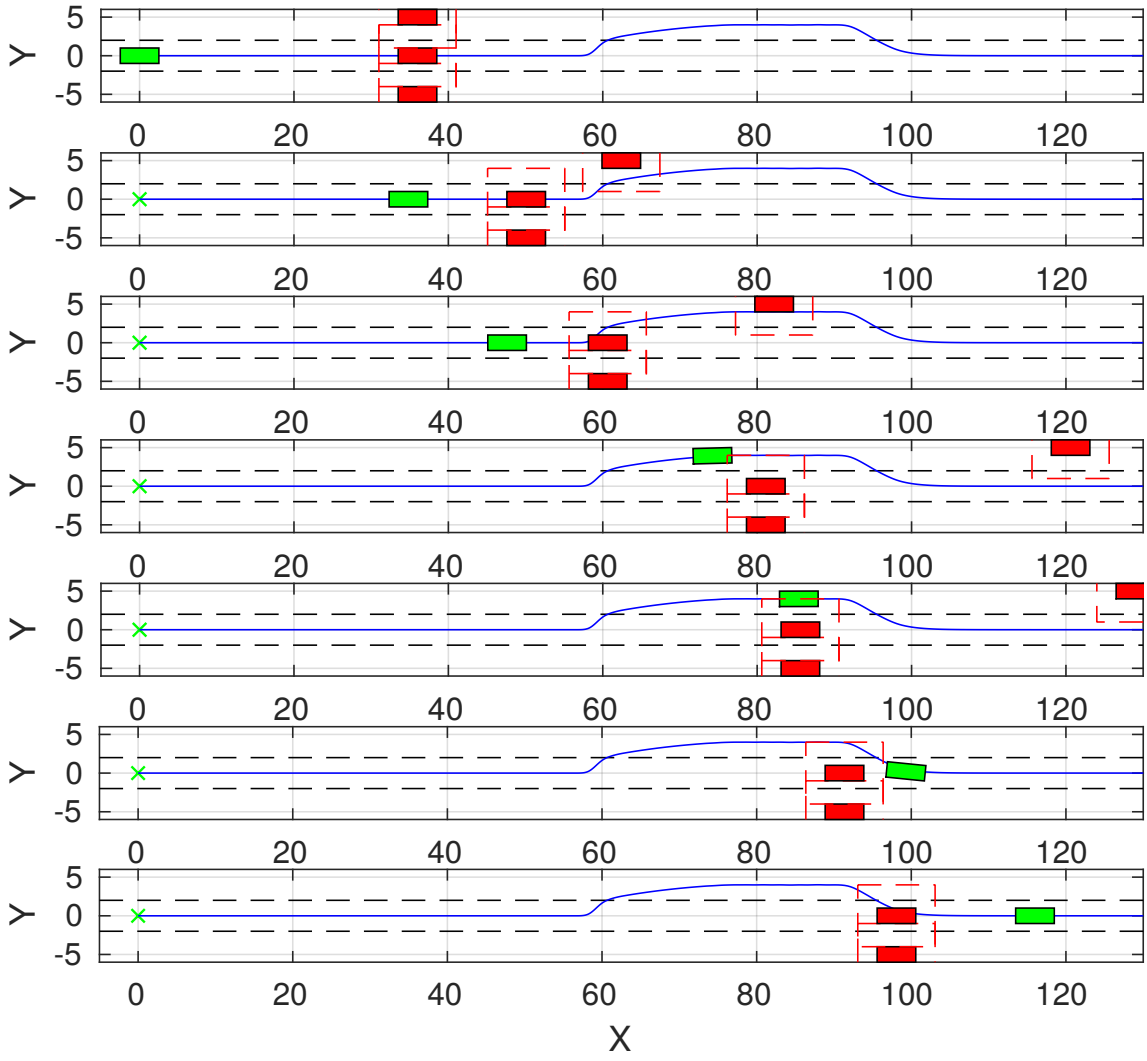

Figure 4.8: Simulation of braking and overtaking obstacles.

a free lane. In the first part of the simulation, the ATLASCAR2 brakes because there is not enough space for overtaking the cars as shown in Fig. 4.9a. A collision would happen if the vehicle continues to follow the initially planned path with the reference velocity. It is possible to notice that the speed decreases because the applied throttle is negative, so a consistent deceleration is set after $\approx 1.5\,\mathrm{s}$ as depicted in Fig. 4.9b. The velocity of the ATLASCAR2 for $\approx 2\,\mathrm{s}$ adapts to that of the closest obstacle. After a few seconds the fastest car moves and makes available the left lane for overtaking. Dramatic changes of steering angle in early stage are observed in Fig. 4.9c and consequently also on the heading angle in Fig. 4.9d. Then, the ATLASCAR2 returns to the reference velocity during the overtaking of the two obstacles (the applied throttle after $\approx 5\,\mathrm{s}$ is positive). It is seen that the ATLASCAR2 avoids the obstacles and returns to the road center line with a low overshoot.

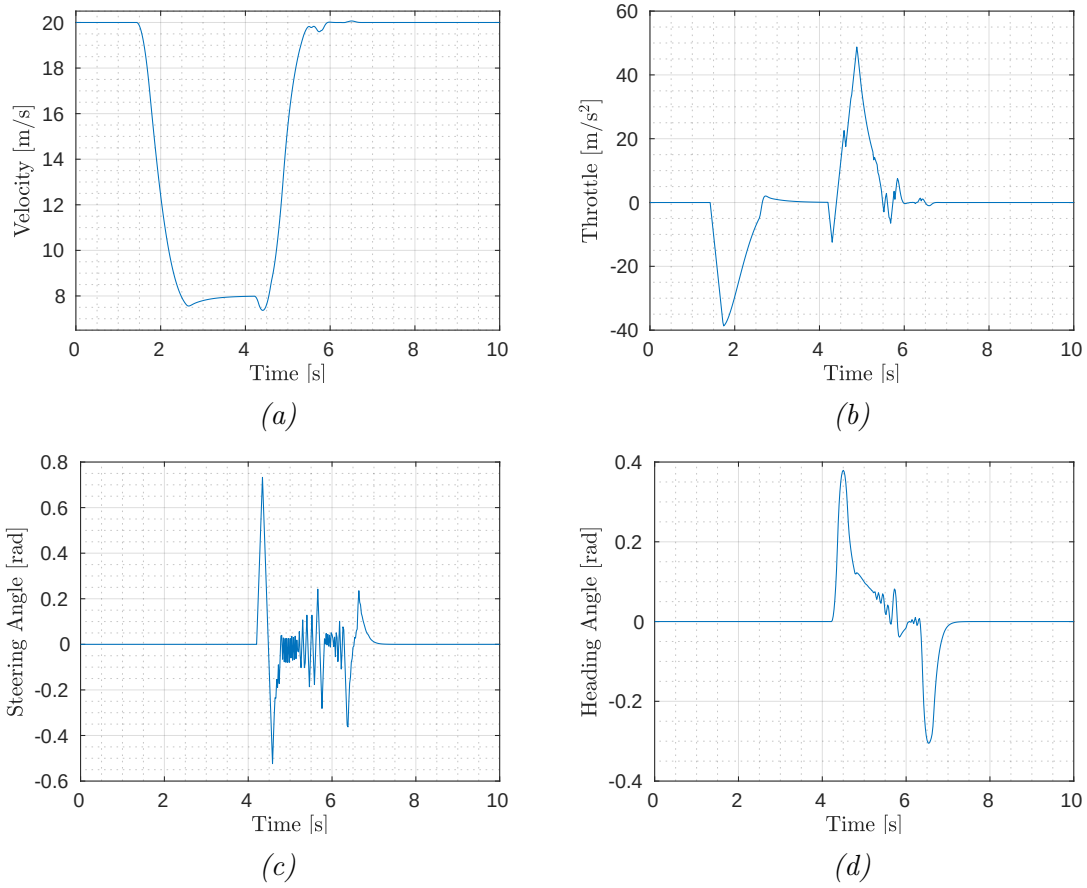

Figure 4.9: Time signals of the ATLASCAR2 in the simulation of braking and overtaking in the situation illustrated in Figure 4.8.

Chapter 5

Lane Following

5.1 Problem Formulation

A lane-following system is a control system that keeps the vehicle traveling along the centerline of a highway lane, while maintaining a user-set velocity. Figure 5.1 illustrates a typical lane following scenario.

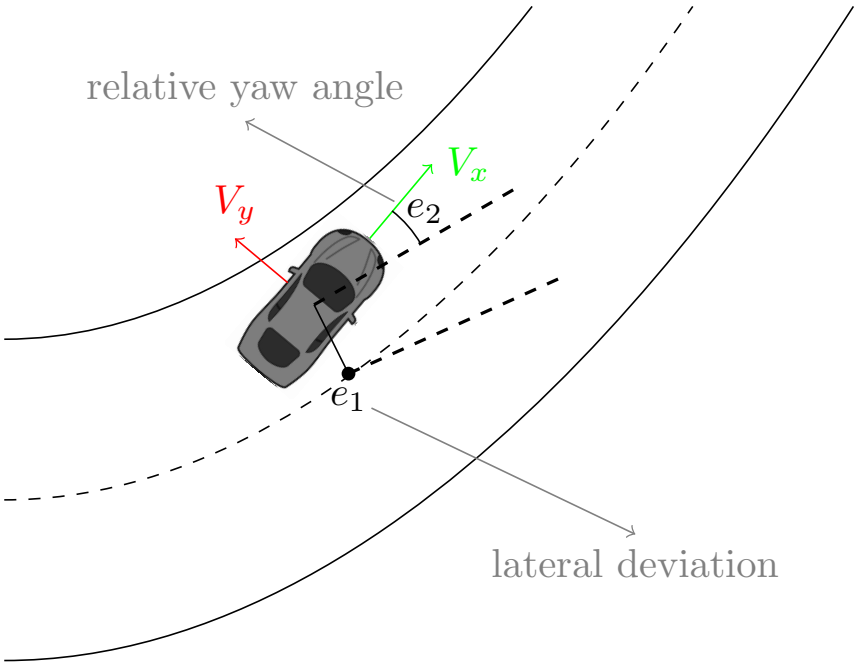

Figure 5.1: Problem description of a lane following system.

In a classic lane keeping assist, it is assumed that the longitudinal velocity is constant [25]. This restriction is relaxed in this model because the longitudinal acceleration varies in this MIMO control system. This lane-following system manipulates both the longitudinal acceleration and the front steering angle of the vehicle to keep the lateral deviation and the relative yaw angle small and the longitudinal velocity close to a driver set velocity. If these two goals cannot be met at the same moment, the system tries to balance them. The model that we are considering contains many parameters. The first fundamental block describes the vehicle dynamics: we have applied the bicycle model of lateral vehicle dynamics and approximate the longitudinal dynamics using a time constant obtaining a linear model.

5.1.1 Longitudinal Dynamics

We can use the following state space to describe the longitudinal model:

$$\begin{aligned} \dot{\boldsymbol{x}}_{\text{lon}} &= \boldsymbol{A}_m \boldsymbol{x}_{\text{lon}} + \boldsymbol{B}_m \boldsymbol{u}_{\text{lon}} \\ \boldsymbol{y}_{\text{lon}} &= \boldsymbol{C}_m \boldsymbol{x}_{\text{lon}} + \boldsymbol{D}_m \boldsymbol{u}_{\text{lon}} \end{aligned} \tag{5.1}$$

where the input is the acceleration and the states are the longitudinal velocity and the actual acceleration which is also the only output of this system.

$$\boldsymbol{x}_{\text{lon}} = \begin{bmatrix} \dot{V}_x \\ V_x \end{bmatrix}, \qquad \boldsymbol{u}_{\text{lon}} = a \tag{5.2}$$

and

$$\begin{aligned} \boldsymbol{A_m} &= \begin{bmatrix} -\frac{1}{\tau} & 0 \\ 1 & 0 \end{bmatrix}, \qquad \boldsymbol{B_m} = \begin{bmatrix} \frac{1}{\tau} \\ 0 \end{bmatrix}, \\ \boldsymbol{C_m} &= \begin{bmatrix} 1 & 0 \end{bmatrix}, \qquad \boldsymbol{D_m} = 0. \end{aligned} \tag{5.3}$$

where τ is a time constant [26]; in practice we are considering a second order transfer function like in [27].

5.1.2 Lateral Dynamics

Local function: we have a continuous vehicle lateral model from parameters obtained by simplifying the one in [28]:

$$\begin{aligned} \dot{\boldsymbol{x}}_{\text{lat}} &= \boldsymbol{A}_g \boldsymbol{x}_{\text{lat}} + \boldsymbol{B}_g \boldsymbol{u}_{\text{lat}} \\ \boldsymbol{y}_{\text{lat}} &= \boldsymbol{C}_g \boldsymbol{x}_{\text{lat}} + \boldsymbol{D}_g \boldsymbol{u}_{\text{lat}} \end{aligned} \tag{5.4}$$

where the input is the steering angle in radians, and the outputs are the lateral velocity in meters per second and yaw angle rate in radians per second:

$$\boldsymbol{x}_{\text{lat}} = \begin{bmatrix} V_y \\ \dot{\psi} \end{bmatrix} \qquad \boldsymbol{u}_{\text{lat}} = \delta \tag{5.5}$$

and

$$\boldsymbol{A}_g = \begin{bmatrix} -\dfrac{2C_F + 2C_R}{mV_x} & -\dfrac{2C_F l_F - 2C_R l_R}{mV_x} - V_x \\ -\dfrac{2C_F l_F - 2C_R l_R}{I_Z V_x} & -\dfrac{2C_F l_F^2 + 2C_R l_R^2}{I_Z V_x} \end{bmatrix}, \tag{5.6}$$

$$\boldsymbol{B}_g = \begin{bmatrix} 2C_F/m \\ 2C_F l_F / I_Z \end{bmatrix}, \qquad \boldsymbol{C}_g = \begin{bmatrix} 1 & 0 \\ 0 & 1 \end{bmatrix} = \boldsymbol{I}_2, \qquad \boldsymbol{D}_g = \begin{bmatrix} 0 \\ 0 \end{bmatrix} = \boldsymbol{0}_{2\times 1}.$$

The parameters in the previous matrices are:

- V_x is the longitudinal velocity of the car;
- m is the total mass parameter;
- I_Z is the yaw moment of inertia parameter;
- l_F and l_R are the longitudinal distances from center of gravity to front and rear tires parameters;
- C_F and C_R are the cornering stiffnesses of front and rear tires parameters.

5.1.3 Augmented Model for Lateral Dynamics

The goal for the driver steering model is to keep the vehicle in its lane and follow the curved road by controlling the front steering angle . This goal is achieved by driving the yaw angle error $e_2 = \psi - \psi_{\text{des}}$ and lateral displacement error e_1 to zero ($\dot{e}_1 = V_x e_2 + V_y$). We can incorporate these two paramenters in the augmented model:

$$\begin{aligned} \dot{\boldsymbol{x}}_{\text{aug}} &= \boldsymbol{A}_a \boldsymbol{x}_{\text{aug}} + \boldsymbol{B}_a \boldsymbol{u}_{\text{aug}} \\ \boldsymbol{y}_{\text{aug}} &= \boldsymbol{C}_a \boldsymbol{x}_{\text{aug}} + \boldsymbol{D}_a \boldsymbol{u}_{\text{aug}} \end{aligned} \tag{5.7}$$

where

$$\boldsymbol{x}_{\text{aug}} = \begin{bmatrix} V_y \\ \dot{\psi} \\ e_1 \\ e_2 \end{bmatrix}, \qquad \boldsymbol{u}_{\text{aug}} = \begin{bmatrix} \delta \\ \dot{\psi}_{\text{des}} \end{bmatrix} \tag{5.8}$$

and

$$\begin{gathered} \boldsymbol{A}_a = \begin{bmatrix} \boldsymbol{A}_g & \boldsymbol{0}_{2\times 2} \\ \boldsymbol{I}_2 & \begin{matrix} 0 & V_x \\ 0 & 0 \end{matrix} \end{bmatrix}, \qquad \boldsymbol{B}_a = \begin{bmatrix} \boldsymbol{B}_g & \boldsymbol{0}_{2\times 1} \\ \begin{matrix} 0 & 0 \\ 0 & -1 \end{matrix} \end{bmatrix}, \\ \boldsymbol{C}_a = \begin{bmatrix} \boldsymbol{0}_{2\times 2} & \boldsymbol{I}_2 \end{bmatrix}, \qquad \boldsymbol{D}_a = \boldsymbol{0}_{2\times 2}. \end{gathered} \tag{5.9}$$

5.1.4 Overall Model Dynamics

Combining (5.1) with (5.7) yields the state-space model that characterizes the Model Predictive Controller:

$$\begin{aligned} \dot{\boldsymbol{x}}_{\text{tot}} &= \boldsymbol{A}_f \boldsymbol{x}_{\text{tot}} + \boldsymbol{B}_f \boldsymbol{u}_{\text{tot}} \\ \boldsymbol{y}_{\text{tot}} &= \boldsymbol{C}_f \boldsymbol{x}_{\text{tot}} + \boldsymbol{D}_f \boldsymbol{u}_{\text{tot}} \end{aligned} \tag{5.10}$$

where

$$\boldsymbol{x}_{\text{tot}} = \begin{bmatrix} \boldsymbol{x}_{\text{lon}} \\ \boldsymbol{x}_{\text{aug}} \end{bmatrix} = \begin{bmatrix} \dot{V}_x \\ V_x \\ V_y \\ \dot{\psi} \\ e_1 \\ e_2 \end{bmatrix}, \qquad \boldsymbol{u}_{\text{tot}} = \begin{bmatrix} \boldsymbol{u}_{\text{lon}} \\ \boldsymbol{u}_{\text{aug}} \end{bmatrix} = \begin{bmatrix} a \\ \delta \\ \dot{\psi}_{\text{des}} \end{bmatrix} \tag{5.11}$$

and

$$\begin{gathered} \boldsymbol{A}_f = \begin{bmatrix} \boldsymbol{A}_m & \boldsymbol{0}_{2\times 4} \\ \boldsymbol{0}_{4\times 2} & \boldsymbol{A}_a \end{bmatrix}, \qquad \boldsymbol{B}_f = \begin{bmatrix} \boldsymbol{B}_m & \boldsymbol{0}_{2\times 2} \\ \boldsymbol{0}_{4\times 1} & \boldsymbol{B}_a \end{bmatrix}, \\ \boldsymbol{C}_f = \begin{bmatrix} \boldsymbol{C}_m & \boldsymbol{0}_{1\times 4} \\ \boldsymbol{0}_{2\times 2} & \boldsymbol{C}_a \end{bmatrix}, \qquad \boldsymbol{D}_f = \boldsymbol{0}_{3\times 3}. \end{gathered} \tag{5.12}$$

However the system to be controlled is usually modeled by a linear discrete state-space model:

$$\begin{aligned} \boldsymbol{x}_{\text{tot}}(k+1) &= \boldsymbol{A}\boldsymbol{x}_{\text{tot}}(k) + \boldsymbol{B}\boldsymbol{u}_{\text{tot}}(k) \\ \boldsymbol{y}_{\text{tot}}(k) &= \boldsymbol{C}\boldsymbol{x}_{\text{tot}}(k) + \boldsymbol{D}\boldsymbol{u}_{\text{tot}}(k) \end{aligned} \tag{5.13}$$

where $\boldsymbol{A}$ and $\boldsymbol{B}$ are the state and control matrices for the discrete state-space equation, respectively, which can be calculated, also in this case, with the Euler

method as:

$$\boldsymbol{A} = e^{\boldsymbol{A}_f T_s}, \qquad \boldsymbol{B} = \int_{kT_s}^{(k+1)T_s} e^{\boldsymbol{A}_f[(k+1)T_s - \eta]} \boldsymbol{B}_f d\eta$$

where T_s is the sampling interval for the discrete state-space model. The matrices $\boldsymbol{C}$ and $\boldsymbol{D}$ are equivalent to those in the continuous case.

5.2 Design of Adaptive Model Predictive Control

We created an Adaptive MPC controller with a prediction model that has six states, three outputs (longitudinal velocity, lateral deviation, relative yaw angle), and two manipulated signals (acceleration and steering). The objective of the trajectory planning along specified path can be described as follows: given a path which the vehicle is expected to follow design a trajectory of a car-vehicle configuration. In order to do this, according with [29] it is possible to derive the road curvature and its derivative. The product of the road curvature and the longitudinal velocity is modeled as a measured disturbance. We have set the constraints for manipulated variables and the scale factors. Moreover we have specified the weights in the standard MPC cost function. The third output, yaw angle, is allowed to float because there are only two manipulated variables to make it a square system. In this controller, there is no steady-state error in the yaw angle as long as the second output, lateral deviation, reaches 0 at steady state. Finally we have also penalized acceleration change more for smooth driving experience. This controller uses a linear model for the vehicle dynamics and updates the model online as the longitudinal velocity varies.

5.3 Simulation Results

The proposed adaptive MPC algorithm is designed in the MATLAB/Simulink and validated through different simulations. The objective of these test is to evaluate the behavior of the proposed control strategy in critical situations. Table 3 shows the parameters used in the lane following simulations.

Parameters	Values
m	1575 kg
I_z	2875 kgm^2
l_F	1.2 m
l_R	1.6 m
C_F	19 000 N/rad
C_R	33 000 N/rad
τ	0.2
V_0	15 m/s
V_{set}	20 m/s
T_s	0.02 s

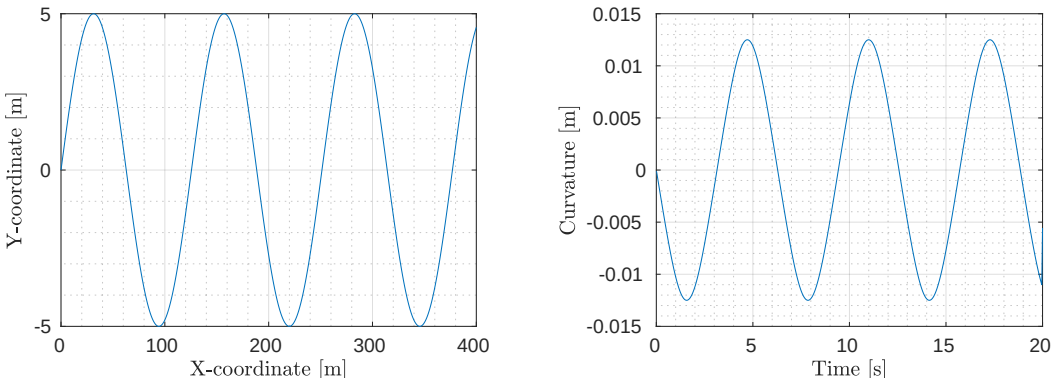

(a) *(b)*

Figure 5.2: Desired path and curvature of the ATLASCAR2 in a simulation of 20 s.

5.3.1 Sinusoidal Path

Figures 5.2a and 5.2b show the desired path that the car must follow and its curvature, where the former is described in terms of the lateral position Y_{ref} as function of the longitudinal position X_{ref} and the latter is derived according with [29]. The ATLASCAR2 is controlled to follow a sinusoidal trajectory which is given as follows:

$$X_{\text{ref}} = V_x \cdot t, \quad Y_{\text{ref}} = 5\sin(X_{\text{ref}}/20) \quad \text{with} \quad t \in [0, 20]\text{s} \tag{5.14}$$

Moreover the following figures show the trend of the main parameters confirming that the control strategy used allows the vehicle to follow the path. In particular we simulated also a small error in the sensor dynamics in order to make the simulation more realistic: we added a 3 percent error to the longitudinal velocity and this is evident from the small noise in the graphs of the steering angle (Figure 5.3c) and the lateral deviation (Figure 5.3e). Figure 5.3a shows the evolution of the vehicle longitudinal velocity. At the start of the simulation, this velocity is equal to the initial condition for longitudinal velocity parameter V_0. At run time, we can note that V_x reaches the predefined value of 20 m/s and then it stabilizes near the cruising speed because it continues to vary the steering angle to adapt to the path to be followed. Finally we presents the overall scheme for the lane following developted in Simulink depicted in Figure 5.4.

5.3.2 Simple Curve Path

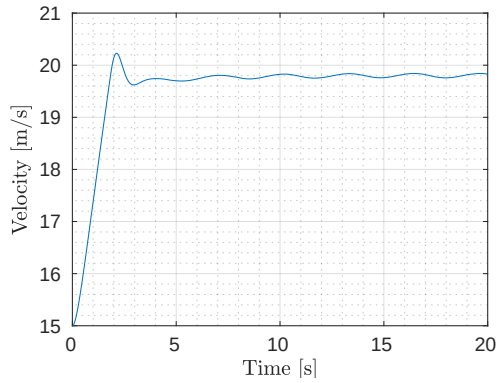

(a) Longitudinal velocity V_x w.r.t. time.

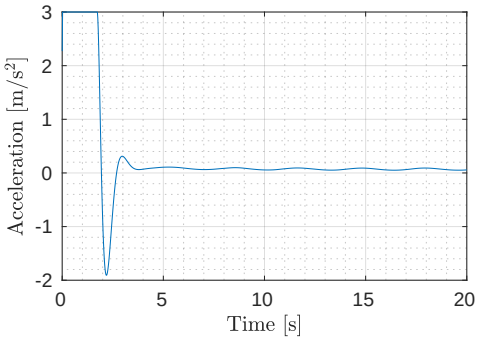

(b) Acceleration u_1 w.r.t. time.

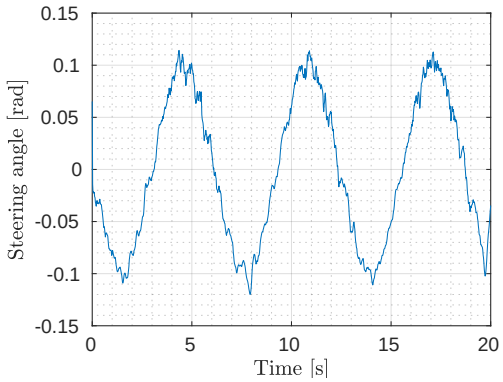

(c) Steering angle u_2 w.r.t. time.

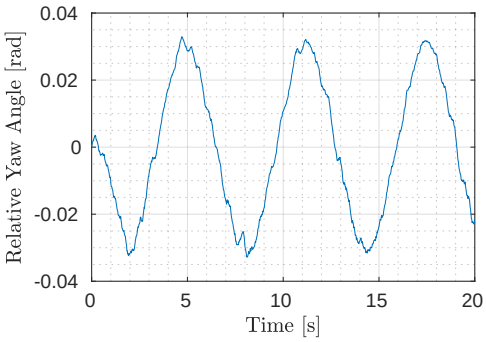

(d) Relative yaw angle e_2 w.r.t. time.

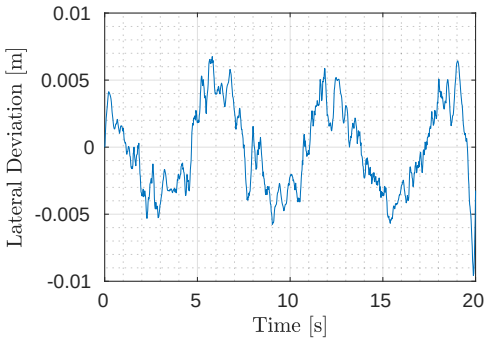

(e) Lateral deviation e_1 w.r.t. time.

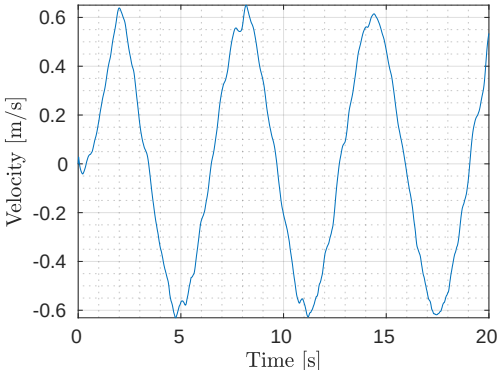

(f) Lateral velocity V_y w.r.t. time.

Figure 5.3: Time signals of the ATLASCAR2 in the simulation with a sinusoidal path.

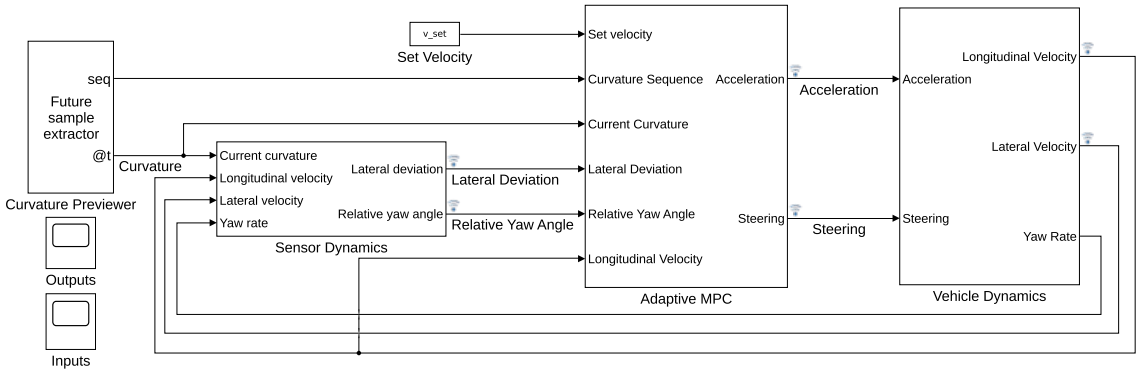

Figure 5.4: Overall procedure scheme lane following.

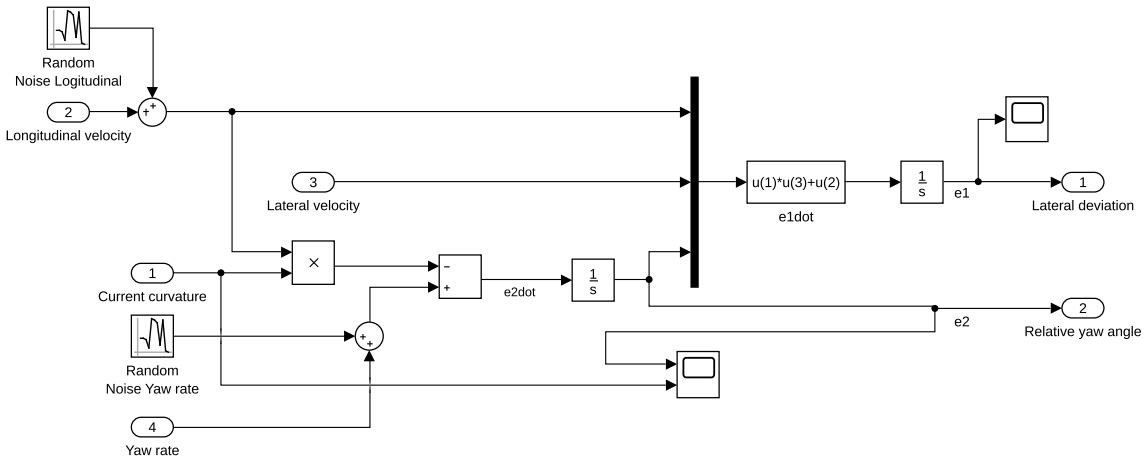

Figure 5.5: Sensor Dynamics of the overall scheme lane following.

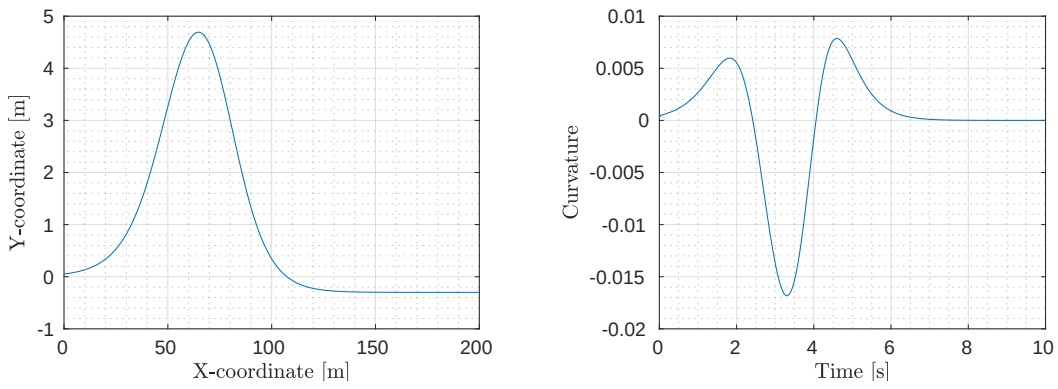

(a) *(b)*

Figure 5.6: Desired path and curvature of the ATLASCAR2 in a simulation of 10 s.

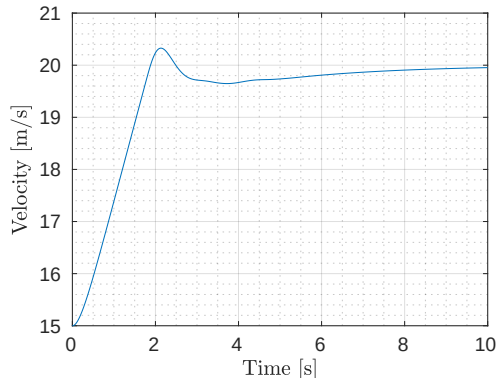

(a) Longitudinal velocity V_x w.r.t. time.

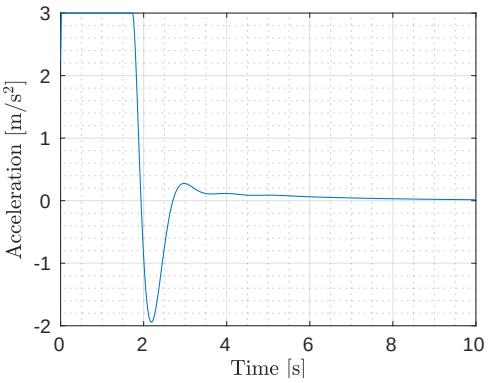

(b) Acceleration u_1 w.r.t. time.

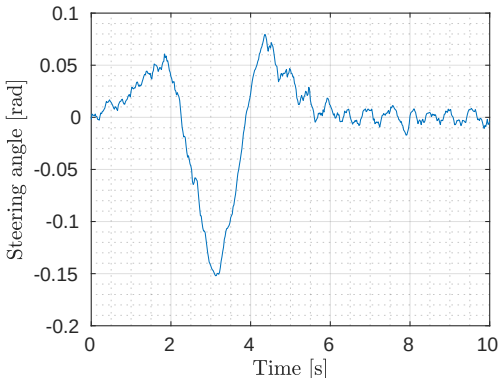

(c) Steering angle u_2 w.r.t. time.

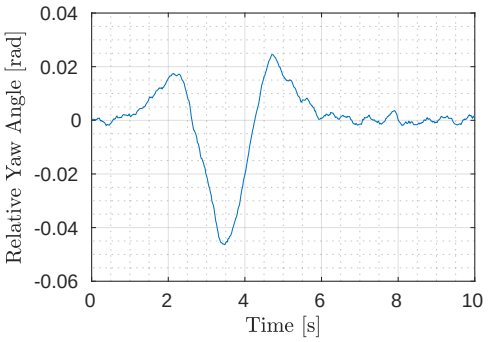

(d) Relative yaw angle e_2 w.r.t. time.

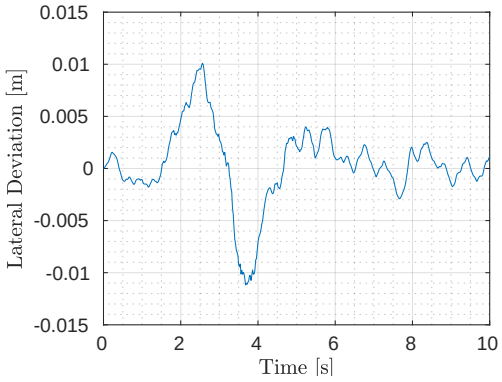

(e) Lateral deviation e_1 w.r.t. time.

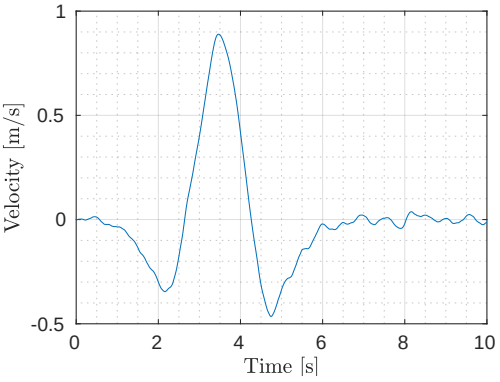

(f) Lateral velocity V_y w.r.t. time.

Figure 5.7: Time signals of the ATLASCAR2 in the simulation with a curve path.

Conclusions and Future Work

This thesis proposes two advanced methods for short term motion planning of an autonomous car based on adaptive Model Predictive Control. The first component is an obstacle avoidance system that moves the vehicle around different moving obstacles in the lane using throttle and steering angle. This system updates both the predictive model and the mixed input/output constraints at each control interval. The vehicle is also able to brake in order to prevent collisions against closest obstacles. Instead, in the second scheme we have developed a lane following system that keeps the ATLASCAR2 traveling along the centerline of the lanes on the road by adjusting the front steering angle of the car. The flexibility of the concepts used in the algorithms allows a multitude of refinements and extensions to this work. The future work includes the combination of these two control strategies in a way that they can operate simultaneously. In order to achieve this objective we have started to simulate a trajectory tracking framework using a slight modification of the linearized tracking error model in [30]. Next expected steps include the migration to ROS-Gazebo simulation environment and, later on, the usage of real data collected on board the ATLASCAR2 and, ultimately, test it in a real autonomous driving scenario.

Bibliography

[1] J. F. Pereira, "Estacionamento autónomo usando perceção 3D Autonomous parking using 3D perception," dissertação de mestrado, Departamento de Engenharia Mecânica, Universidade de Aveiro, 2012.

[2] R. Silva, "ATLASCAR2 Local Navigation for Autonomous Driving and Driver Assistance," Master's thesis, Universidade de Aveiro, Aveiro, 2018.

[3] A. Broggi, M. Buzzoni, S. Debattisti, P. Grisleri, M. C. Laghi, P. Medici, and P. Versari, "Extensive tests of autonomous driving technologies," *IEEE Transactions on Intelligent Transportation Systems*, vol. 14, no. 3, pp. 1403–1415, 2013.

[4] A. Bemporad, M. Morari, N. L. Ricker, and H. T. C. Mathworks, "Model predictive control toolbox: Getting started guide, the math works."

[5] B. Siciliano, L. Sciavicco, L. Villani, and G. Oriolo, *Robotics: Modelling, Planning and Control*. Springer Publishing Company, Incorporated, 1st ed., 2008.

[6] J. Skoda, "3D Navigation for Mobile Robots," Master's thesis, Charles University, Prague, 2016.

[7] J. Bai, "Robot Navigation Using Velocity Potential Fields and Particle Filters for Obstacle Avoidance," Master's thesis, University of Ottawa, Ottawa, 2015.

[8] D. Gruyer, V. Magnier, K. Hamdi, L. Claussmann, O. Orfila, and A. Rakotonirainy, "Perception, information processing and modeling: Critical stages for autonomous driving applications," *Annual Reviews in Control*, vol. 44, pp. 323–341, 2017.

[9] W. H. O. WHO, *Global Status Report on Road Safety 2015*. Nonserial Publication, World Health Organization, 2015.

[10] C. Katrakazas, M. Quddus, W. H. Chen, and L. Deka, "Real-time motion planning methods for autonomous on-road driving: State-of-the-art and future research directions," *Transportation Research Part C: Emerging Technologies*, vol. 60, pp. 416–442, 2015.

[11] V. Santos, J. Almeida, E. Avila, D. Gameiro, M. Oliveira, R. Pascoal, R. Sabino, and P. Stein, "ATLASCAR - technologies for a computer assisted driving system on board a common automobile," in *13th International IEEE Conference on Intelligent Transportation Systems, Funchal, Madeira, Portugal, 19-22 September 2010*, pp. 1421–1427, 2010.

[12] R. F. Cabral de Azevedo, "Sensor Fusion of LASER and Vision in Active Pedestrian Detection," dissertação de mestrado, Departamento de Engenharia Mecânica, Universidade de Aveiro, 2014.

[13] D. T. Vieira da Silva, "Calibração Multissensorial e Fusão de Dados Utilizando LIDAR e Visão," dissertação de mestrado, Departamento de Engenharia Mecânica, Universidade de Aveiro, 2016.

[14] J. D. Madureira Correia, "Unidade de Perceção Visual e de Profundidade Para o Atlascar2," dissertação de mestrado, Departamento de Engenharia Mecânica, Universidade de Aveiro, 2017.

[15] K. Bimbraw, "Autonomous Cars: Past, Present and Future - A Review of the Developments in the Last Century, the Present Scenario and the Expected Future of Autonomous Vehicle Technology," *Proceedings of the 12th International Conference on Informatics in Control, Automation and Robotics*, no. August, pp. 191–198, 2015.

[16] Waymo, "Waymo - journey," 2018.

[17] Waymo, "Waymo - technology," 2018.

[18] A. Broggi, P. Medici, E. Cardarelli, P. Cerri, A. Giacomazzo, and N. Finardi, "Development of the control system for the vislab intercontinental autonomous challenge," in *13th International IEEE Conference on Intelligent Transportation Systems*, pp. 635–640, Sep. 2010.

[19] R. Zhang and M. Pavone, "Control of robotic mobility-on-demand systems: A queueing-theoretical perspective," *The International Journal of Robotics Research*, vol. 35, no. 1-3, pp. 186–203, 2016.

[20] V. Santos, "ATLASCAR: A sample of the quests and concerns for autonomous cars," in *Informatics in Control, Automation and Robotics: 14th International Conference, ICINCO 2017 Madrid, Spain, July 26-28, 2017 Revised Selected Papers* (O. Gusikhin and K. Madani, eds.), Lecture Notes in Electrical Engineering, Springer International Publishing, 2019.

[21] Y. Kuwata, G. A. Fiore, J. Teo, E. Frazzoli, and J. P. How, "Motion planning for urban driving using rrt," in *2008 IEEE/RSJ International Conference on Intelligent Robots and Systems*, pp. 1681–1686, Sep. 2008.

[22] Y. Gao, T. Lin, F. Borrelli, E. Tseng, and D. Hrovat, "Predictive control of autonomous ground vehicles with obstacle avoidance on slippery roads," 01 2010.

[23] T. Xu and H. Yuan, "Autonomous vehicle active safety system based on path planning and predictive control," in *2016 35th Chinese Control Conference (CCC)*, pp. 8889–8895, July 2016.

[24] W. Xi and J. S. Baras, "Mpc based motion control of car-like vehicle swarms," in *2007 Mediterranean Conference on Control Automation*, pp. 1–6, June 2007.

[25] M. Bujarbaruah, X. Zhang, H. E. Tseng, and F. Borrelli, "Adaptive MPC for autonomous lane keeping," *CoRR*, vol. abs/1806.04335, 2018.

[26] Y. Wang, Y. Bin, and K. Li, "Longitudinal acceleration tracking control of low speed heavy-duty vehicles," *Tsinghua Science and Technology*, vol. 13, pp. 636–643, Oct 2008.

[27] J. Filip, *Trajectory Tracking for Autonomous Vehicles*. PhD thesis, 05 2018.

[28] K. Murali Madhavan Rathai, J. Amirthalingam, and B. Jayaraman, "Robust tube-mpc based lane keeping system for autonomous driving vehicles," pp. 1–6, 06 2017.

[29] and, "Trajectory planning for a four-wheel-steering vehicle," in *Proceedings 2001 ICRA. IEEE International Conference on Robotics and Automation (Cat. No.01CH37164)*, vol. 4, pp. 3320–3325 vol.4, May 2001.

[30] H. Yang, M. Guo, Y. Xia, and L. Cheng, "Trajectory tracking for wheeled mobile robots via model predictive control with softening constraints," *IET Control Theory Applications*, vol. 12, no. 2, pp. 206–214, 2018.